Catalysis Today xxx (2015) xxx–xxx

Contents lists available at ScienceDirect

Catalysis Today

journal homepage: www.elsevier.com/locate/cattod

The effect of UTL layer connectivity in isoreticular zeolites on the catalytic performance in toluene alkylation

Naděžda Žilková[a], Pavla Eliášová[a], Sulaiman Al-Khattaf[b], Russell E. Morris[c], Michal Mazur[a], Jiří Čejka[a,b,*]

[a] J. Heyrovský Institute of Physical Chemistry, Academy of Sciences of the Czech Republic, v.v.i., 182 23 Prague 8, Czech Republic
[b] Centre of Research Excellence in Petroleum Refining and Petrochemicals, King Fahd University of Petroleum & Minerals, Dhahran 31261, Saudi Arabia
[c] EaStCHEM School of Chemistry, University of St. Andrews, St. Andrews KY16 9ST, United Kingdom

ARTICLE INFO

Article history:
Received 4 August 2015
Received in revised form 8 September 2015
Accepted 10 September 2015
Available online xxx

Keywords:
UTL
ADOR zeolites
PCR
OKO
Toluene alkylation
IPC zeolites

ABSTRACT

Toluene alkylation with isopropyl alcohol was used as a model reaction to investigate the effect of UTL-type layer connectivity in a series of isoreticular zeolites and related zeolitic materials. All prepared catalysts possess the same structure of the layers but their connectivity differs from amorphous pillars (IPC-1PI), double-four-rings (UTL), single-four-rings (IPC-2 = OKO, International Zeolite Association code), oxygen bridges (IPC-4 = PCR), or their combinations (IPC-6 and IPC-7). X-ray powder diffraction, scanning electron microscopy, and nitrogen adsorption isotherms were employed to characterize structural and textural properties of the studied catalysts. Deuterated acetonitrile was adsorbed on catalysts to determine the concentrations and type of individual acid sites. Toluene alkylation with isopropyl alcohol evidenced that toluene conversion increases with increasing size of zeolite channels. Simultaneously, selectivity in cymenes increased as open structure of these catalysts did not present optimum reaction volume for the bimolecular reaction of cymenes with toluene to *n*-propylbenzenes.

1. Introduction

Zeolites are the most important catalysts not only due to their large-scale applications but also as model catalysts for different types of reactions [1–3]. Activity and selectivity of zeolites are straightforwardly related to the size and connectivity of channels in a zeolite framework and to their chemical composition, controlling the type, concentration, location, and strength of acid sites. To tailor both textural and chemical properties of zeolites, many different approaches have been proposed [4–7].

Recently, we have developed a novel methodology for the zeolite synthesis based on a top-down protocol called ADOR (Assembly–Disassembly–Organisation–Reassembly) [8]. This new synthetic protocol includes synthesis of an appropriate zeolite (A), its chemically selective decomposition with preservation of the individual UTL layers (D), organization of the layers (O), and last but not least their reassembly by condensation providing a new zeolite (R). It was exemplified on germanosilicate UTL, which can be chemically and regio-selectively hydrolysed into IPC-1P layered material [8,9]. The nanosheets preserve the original UTL layer structure and they are connected together only via a net of hydrogen bonds [10,11]. Several post-synthetic treatments were proposed to adjust the interlayer distance and to manipulate the individual layers [9,12–14]. When optimized conditions are applied, several new zeolites can be synthesized possessing the same intra-layer connectivity but differing in how the layers are joined together, caused by controllable introduction of connecting units like double-four-ring (D4R), single-four-ring (S4R), and/or oxygen bridges [8]. This family of zeolites forms an isoreticular series; a set of materials with the same overall topological features but different size pores. This shows that substantial extension of zeolite structures can be achieved by using relatively labile zeolites like germanosilicate UTL and application of the ADOR protocol [6]. The ADOR principal was demonstrated also on other germanosilicates, e.g. IWW, ITH, ITR, IWR [15,16], and overviewed in the recently published review paper [8].

This contribution is focused on the catalytic behaviour of a series of zeolites prepared from parent UTL and having the same (UTL) layer topology but different inter-layer connectivity. Table 1 addresses zeolites under investigation and their channel entrances. Toluene alkylation with isopropyl alcohol is followed with respect to toluene conversion, selectivity to cymenes and *n*-propyltoluenes and *para*-selectivity.

* Corresponding author at: J. Heyrovský Institute of Physical Chemistry, Academy of Sciences of the Czech Republic, 182 23 Prague 8, Czech Republic.
E-mail address: jiri.cejka@jh-inst.cas.cz (J. Čejka).

http://dx.doi.org/10.1016/j.cattod.2015.09.033
0920-5861/

Table 1
Structural parameters of zeolites derived from germanosilicate UTL and studied in this paper. In the structure figures the blue points represent the connecting units or amorphous SiO_2 in the case of IPC-1PI, while red points indicate the intra-layer atoms (* D4R = double-four-ring, S4R = single-four-ring).

Zeolite structure	Connecting unit(s)*	Channel size in angstroms (Å)					
		14-ring	12-ring	12-ring	10-ring	10-ring	8-ring
UTL 	D4R	9.5 x 7.1	8.5 x 5.5				
IPC-7 	D4R, S4R	9.5 x 7.1	8.5 x 5.5	6.6 x 6.2	5.4 x 5.3		
IPC-2 	S4R			6.6 x 6.2	5.4 x 5.3		
IPC-6 	S4R, oxygen			6.6 x 6.2	5.4 x 5.3	5.8 x 3.8	4.5 x 3.6
IPC-4 	oxygen					5.8 x 3.8	4.5 x 3.6
IPC-1PI 	amorphous SiO_2						

Reactions of aromatic hydrocarbons are not only important industrial processes catalyzed by zeolites but they are frequently used for characterization of zeolites [17–19]. Toluene alkylation with isopropyl alcohol was chosen as a model reaction because selectivities to individual reaction products reflect in a high extent the effect of size and connectivity of the zeolite channel systems [20]. While the first alkylation step provides exclusively isopropyl toluenes, the second reaction step can involve isomerization, secondary alkylation but also bimolecular transalkylation between isopropyl toluene and toluene. This reaction is of a particular importance as it proceeds mostly in 10-ring (10-R) intersecting channels and thus it can provide a valuable information about the zeolite channel intersections [21].

2. Experimental

2.1. Material synthesis

Zeolites MFI and BEA used as commercial catalysts were purchased from Zeolyst and used after four-times repeated ion-exchange with 0.5 M NH_4NO_3 solution.

Zeolite UTL containing aluminium was prepared according to the procedure described in the literature [22]. The pure germanosilicate UTL was prepared according to Refs. [22,23] and used as the starting material for the post synthesis alumination of IPC zeolites according to the following procedure. 1 g of calcined UTL (with Si/Ge molar ratio 4.4) was hydrolysed with the mixture of 150 ml 1 M CH_3COOH and 100 ml 0.5–2 M $Al(NO_3)_3$. The mixture was stirred under reflux at 85–95 °C for 16 h. The solid was filtered and thoroughly washed with water and 0.1 M HCl. The resultant aluminated IPC-1P was used for the synthesis of IPC-1PI, IPC-2 and IPC-4 as follows:

- For the synthesis of IPC-1PI, 1 g of IPC-1P was first swollen with 20 ml of 20 wt% cetyltrimethylammonium hydroxide solution (C_{16}TMA-OH) by stirring at ambient temperature for 16 h. The IPC-1SW was then treated with TEOS (for 1 g of zeolite 50 ml TEOS) at 85 °C for 16 h. The resulted solid was hydrolysed in water and then calcined at 550 °C for 6 h. For more details see Ref. [24].
- For the synthesis of IPC-2, 1 g of IPC-1P was heated with 10 g of 1 M HNO_3 and 0.2 g of diethoxydimethysilane at 175 °C for 16 h and subsequently calcined at 650 °C for 6 h [9].
- For the synthesis of IPC-4, 1 g of IPC-1P was treated with 13.5 g of neat octylamine at 60 °C for 16 h and subsequently calcined at 650 °C for 6 h [9].

IPC-6 was prepared in two following steps: 1 g of calcined UTL (with Si/Ge ratio 4.4) was hydrolysed with 150 ml of 1 M CH_3COOH and 100 ml of 1.6 M $Al(NO_3)_3$ at 85 °C for 16 h. The solid was filtered, washed with water, dried and subsequently treated with octylamine (per 1 g of zeolite 13.5 g of octylamine) at 60 °C for 16 h. The final product was calcined at 650 °C for 6 h.

IPC-7 was prepared in two following steps: 1 g of calcined UTL (with Si/Ge ratio 7.4) was hydrolysed with 100 ml of 3 M $Al(NO_3)_3$ at 80 °C for 2 h. The solid was isolated by filtration, dried and again hydrolysed with 100 ml of 1 M $Al(NO_3)_3$ under the same conditions. The final product was separated by filtration, dried and calcined at 550 °C for 6 h.

2.2. Characterization

The structure and crystallinity of the zeolites were determined by X-ray powder diffraction using a Bruker AXS D8 Advance diffractometer equipped with a graphite monochromator and a position sensitive detector Våntec-1 using Cu Kα radiation in Bragg–Brentano geometry.

Nitrogen adsorption/desorption isotherms were measured on a Micromeritics GEMINI II 2370 volumetric Surface Area Analyzer at −196 °C to determine surface area, pore volume and pore size distribution. Before the sorption measurements, all samples were degassed in a Micromeritics FlowPrep 060 instrument under helium at 300 °C (heating rate 10 °C/min) for 4 h. The specific surface area was evaluated by BET method using adsorption data in the range of a relative pressure from $p/p_0 = 0.05$ to $p/p_0 = 0.25$. The t-plot method was applied to determine the volume of micropores (V_{mic}). The adsorbed amount at relative pressure $p/p_0 = 0.98$ reflects the total adsorption capacity (V_{tot}).

The concentration and the type of acid sites were determined by adsorption of acetonitrile as a probe molecule followed by FTIR spectroscopy (Nicolet 6700 FTIR with DTGS detector) using the self-supported wafer technique. Prior to adsorption of the probe molecule, self-supported wafers of zeolite samples were activated in situ by overnight evacuation at temperature 450 °C. CD_3CN adsorption proceeded at room temperature for 30 min at equilibrium pressure 5 Torr, followed by 30 min degassing at room temperature. To obtain quantitative analysis, the molar absorption coefficients for CD_3CN adsorbed on Brønsted acid sites (ν(C≡N)-B at 2297 cm^{-1}, $\varepsilon(B) = 2.05 \pm 0.1$ cm μmol^{-1}) and strong and weak Lewis acid sites (ν(C≡N)-L_1 at 2325 cm^{-1} ν(CN)-L_2 2310 cm^{-1}, $\varepsilon(L) = 3.6 \pm 0.2$ cm μmol^{-1}) were used [25]. Integral intensities of individual bands were used and spectra were normalized to the wafer thickness 10 mg cm^{-2}.

2.3. Catalytic experiments – toluene alkylation

The catalytic behaviour of novel zeolites was tested in toluene alkylation with isopropyl alcohol and compared with the commercial MFI and BEA zeolites. The reaction was investigated in a down-flow glass micro-reactor with a fixed bed of catalyst under atmospheric pressure. Before the catalytic run, zeolite catalysts were activated at 500 °C in nitrogen stream for 120 min. The alkylation of toluene was performed at 250 °C with toluene to isopropyl alcohol (Tol/*i*-PrOH) molar ratio of 9.6 and WHSV based on toluene equal to 10 h^{-1}. The reaction products were analyzed using an "on-line" gas chromatograph (Agilent 6890 Plus) with flame ionization

Please cite this article in press as: N. Žilková, et al., The effect of UTL layer connectivity in isoreticular zeolites on the catalytic performance in toluene alkylation, Catal. Today (2015), http://dx.doi.org/10.1016/j.cattod.2015.09.033

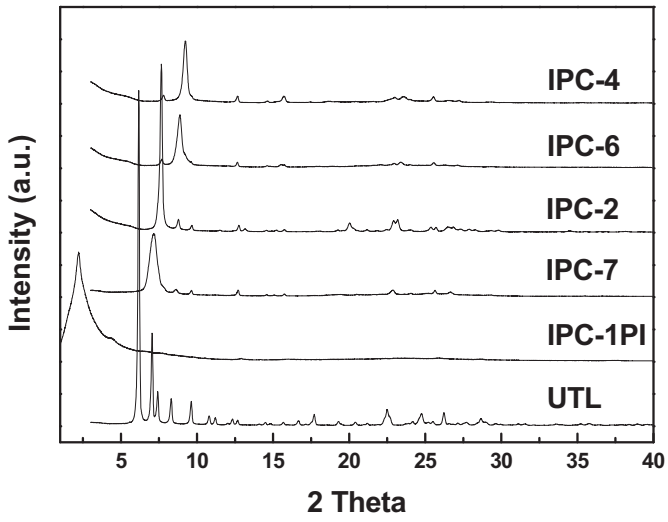

Fig. 1. Powder XRD pattern of UTL zeolite and all IPC zeolites.

detector and a high-resolution capillary column. The first analysis was performed after 15 min of time-on-stream (T-O-S) and the other followed in approx. 55 min interval.

3. Results and discussion

3.1. Characterization of catalysts

In the case of zeolites UTL, IPC-2, IPC-4, IPC-6 and IPC-7 the powder XRD patterns (Fig. 1), adsorption–desorption isotherms (Fig. 2), and SEM images (Fig. 3) evidence the highly crystalline, purely microporous materials without any amorphous phase. Zeolite IPC-2 has the same connectivity but different symmetry as zeolite OKO [26] and zeolite IPC-4 was given the IZA code PCR. Zeolites UTL, IPC-2 and IPC-4 contain only one type of 2-dimensional channel system while zeolites IPC-6 and IPC-7 have a unique combination of two different 2-dimensional pore systems (see Table 1). The common character of the layers in new zeolites is confirmed by the similar profile of intra-layer reflections (Fig. 1). On the other hand, their diversity in the inter-layer connectivity is reflected in the position of the main peak attributed to the inter-layer *d*-spacing. In our materials its position represents the average inter-layer *d*-spacing as some of the zeolites, particularly IPC-6 and IPC-7, have two

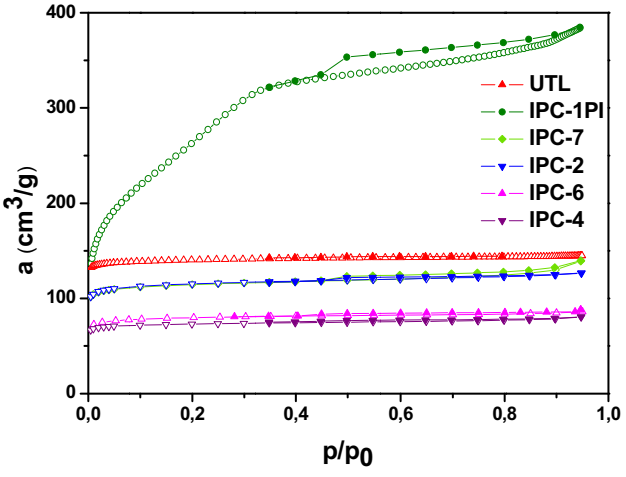

Fig. 2. Adsorption–desorption isotherms of nitrogen measured at −176 °C of investigated zeolites, the solid points denote desorption branch.

distinct inter-layer distances depending on the size and occurrences of connecting unit (see Table 1). With the decreasing average inter-layer distance (from UTL towards IPC-4) the main peak is gradually shifted to higher 2θ values.

UTL and all new zeolites show the same type I of adsorption–desorption isotherms typical for purely microporous materials (Fig. 2). Their micropore volume and the total BET area decrease with the decreasing size of the inter-layer connecting units following the order UTL > IPC-7 ≈ IPC-2 > IPC-6 ≈ IPC-4 (Table 2). In the ideal case, the zeolites are supposed to follow the order UTL (with 100% of D4Rs connections) > IPC-7 (with ~50% of D4Rs ~50% S4Rs) > IPC-2 (with 100% of S4Rs) > IPC-6 (with ~50% of S4Rs and ~50% of oxygen bridges) > IPC-4 (with 100% of oxygen bridges). The similarity in the determined textural properties of IPC-7 vs. IPC-2 and IPC-6 vs. IPC-4 zeolites can be attributed to some local disorder or layer mismatch present in IPC-7 and IPC-6 materials as observed by TEM [27]. Conversely, IPC-2 and IPC-4 are almost perfectly ordered zeolites without any obvious structural defects [9].

On the other hand, the hybrid pillared IPC-1PI material does not exhibit any microporosity but a large mesopore voids created by amorphous SiO_2 pillars in between layers. The silicate layers (of thickness about 0.9 nm) possess neither intra-layer zeolite-like channels nor inter-layer pores. The presence of pillars is clearly detected by an intense reflection in the low angle area in its powder XRD pattern as well as by increased total pore volume (0.594 cm^3/g) and BET area (970 m^2/g) indicating material with highly accessible layer surface (Fig. 2). The specific shape of its isotherm, the steep increase in the nitrogen uptake up to 0.3 p/p_0, indicates the presence of small mesopores with sizes smaller than 4 nm [28,29].

The parent UTL zeolite crystallizes in the ultrathin plate-shape crystals with diameters at least 10 μm × 10 μm and thickness less than 0.1 μm (Fig. 3). The daughter zeolites IPC-2, IPC-4, IPC-6 and IPC-7 exhibit the same crystal morphology and size mostly without any noticeable changes indicating that the hydrolysis conditions and other post-synthetic treatments do not affect the overall crystal morphology. The AFM study confirmed that the zeolites do not undergo the dissolving and recrystallization mechanism during the ADOR protocol [30]. In contrast, the pillared IPC-1PI sample show more aggregated microplates with signs of a partial dissolution as the microplates are broken and slightly damaged (Fig. 3) [31]. This is likely to be caused by the swelling treatment in the highly basic environment.

For the catalytic test, the zeolites were prepared in their aluminosilicate forms. Infrared spectroscopy in combination with d_3-acetonitrile was employed to characterize the type and concentration of acid sites in the catalysts. d_3-Acetonitrile was chosen as a probe molecule as its kinetic diameter allows penetration into the 8-ring channels in contrast to the more frequently used pyridine, which cannot enter 8-ring or certain 10-ring channels.

The infrared spectra of all catalysts after activation at 450 °C and after adsorption desorption cycle with d_3-acetonitrile are depicted in Figs. 4 and 5. Figs. 4A and 5A show typical vibrations of zeolitic materials in hydroxyl region consisting of a band around 3745 cm^{-1} commonly assigned to silanol groups and around 3610–3620 cm^{-1} being characteristic for vibrations of acidic OH groups in Si—OH—Al bridges.

The most intense bands around 3745 cm^{-1} were observed in the case of IPC-1PI and also zeolite Beta. A high concentration of silanol groups is characteristic for pillared materials with amorphous silica pillars, and zeolite Beta also usually possesses a high concentration of these groups. In contrast, the intensity of the band of bridging OH groups depends strongly on the concentration of Al forming Brønsted acid sites.

Adsorption of d_3-acetonitrile resulted in a complete disappearance of Brønsted acid sites, evidences that all sites of this type

Please cite this article in press as: N. Žilková, et al., The effect of UTL layer connectivity in isoreticular zeolites on the catalytic performance in toluene alkylation, Catal. Today (2015), http://dx.doi.org/10.1016/j.cattod.2015.09.033

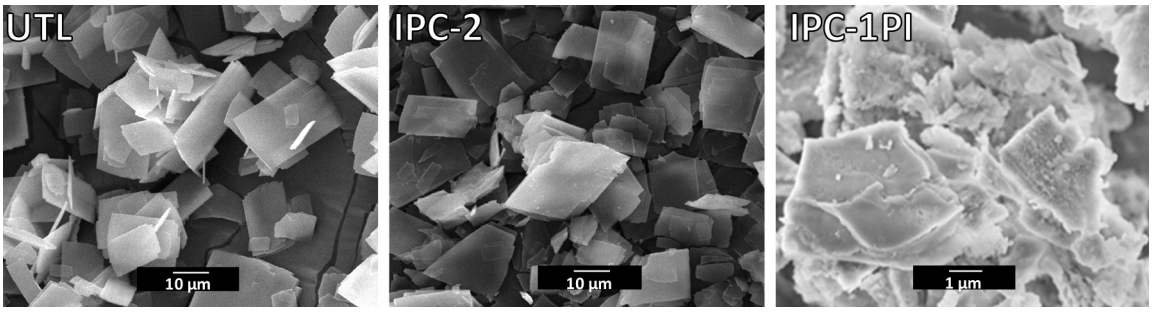

Fig. 3. The SEM pictures of parent UTL zeolite, IPC-2 zeolite representing all daughter's zeolites as their morphology do not substantially change, and the hybrid pillared material IPC-1PI.

Table 2
The physicochemical properties of commercial zeolites and investigated UTL and IPC catalysts.

Material	BET (m^2/g)	V_{total} (cm^3/g)	V_{micro} (cm^3/g)	$c_{Brønsted}$ (mmol/g)[a]	c_{Lewis} (mmol/g)[a]	Si/Al[a]
BEA	619	0.347	0.254	0.330	0.190	23
MFI	423	0.252	0.160	0.287	0.110	32
UTL	560	0.301	0.232	0.037	0.109	64
IPC-1PI	970	0.594	–	0.008	0.089	89
IPC-2	390	0.196	0.159	0.131	0.106	48
IPC-4	247	0.125	0.105	0.080	0.141	45
IPC-6	235	0.113	0.098	0.107	0.165	37
IPC-7	388	0.216	0.160	0.141	0.496	13
IPC-2	375	0.217	0.150	0.074	0.065	81
IPC-2	–	–	–	0.041	0.055	109

[a] Determined based on d_3-*acetonitrile* adsorption studied by FTIR.

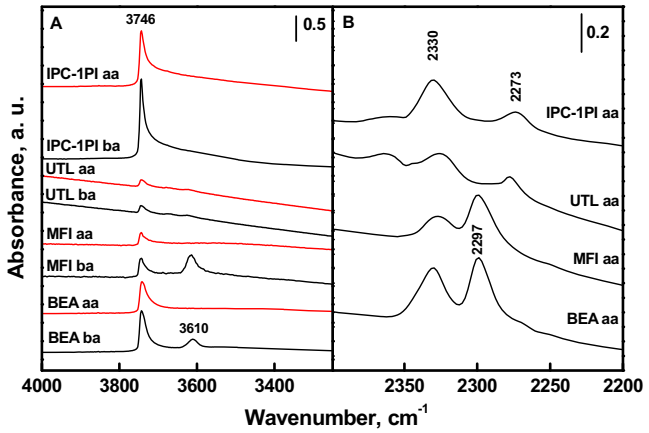

Fig. 4. FTIR spectra of commercial BEA and MFI zeolites, UTL and pillared IPC-1PI before (ba) and after (aa) adsorption of *d*-acetonitrile, region of hydroxyl vibration (A), region of d_3-acetonitrile vibration (B).

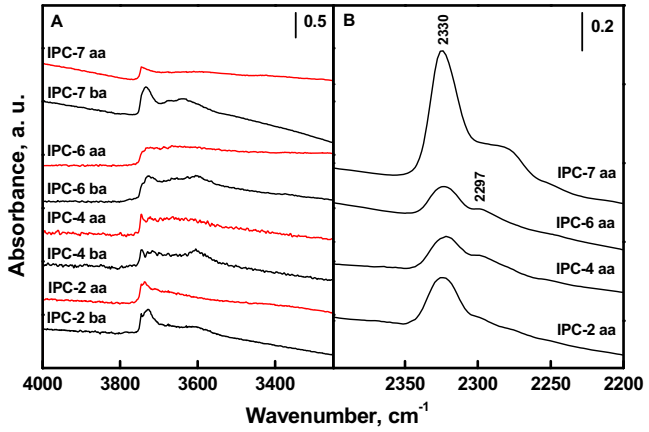

Fig. 5. FTIR spectra of IPC-2 (with Si/Al 48), IPC-4, IPC-6 and IPC-7 before (ba) and after (aa) adsorption of *d*-acetonitrile, region of hydroxyl vibration (A), region of acetonitrile vibration (B).

are accessible for the probe molecule. In contrast, new absorption bands appeared in the area of nitrile groups. Interaction of d_3-acetonitrile with Brønsted acid sites leads to the formation of an absorption band around 2300 cm^{-1} and with Lewis acid sites around 2325–2330 cm^{-1}. In some samples one can also observe a band around 2270–75 cm^{-1} attributed to interaction of d_3-acetonitrile with silanol groups.

Due to the complexity of the synthesis protocols for individual IPC-type catalysts, the concentrations of Al differ in the individual samples and also the Brønsted to Lewis acid site ratio is rather different (Table 2). The parent UTL zeolite can be prepared only with a limited aluminium content [22], here the Si/Al molar ratio was determined to be 64. IPC-2, IPC-4 and IPC-6 zeolites have Si/Al ratio in the range 37–48. The highest aluminium content (Si/Al 13) was detected for IPC-7 zeolite with obvious dominancy of Lewis acids sites. Its FTIR spectrum indicates the presence of some extraframework aluminium. Unlike in other synthetic procedures, the final IPC-7 solid was not washed with HCl solution to remove the extraframework Al species. This step was intentionally omitted because the structure is sensitive to acid solution and the washing with HCl solution may cause unwanted further hydrolysis and structure transformation/decomposition. In most of the prepared zeolites the Lewis acid sites dominate over the Brønsted ones. This is expected as the aluminium was mostly incorporated by post-synthesis treatments during the hydrolysis step when germanium atoms are extracted [32,33].

To study the effect of acid site concentration on the catalytic performance, zeolite IPC-2 was prepared with three different aluminium contents, Si/Al ratios of 48, 81, 109 (see Table 2).

3.2. Toluene alkylation with isopropyl alcohol

Toluene conversions in its alkylation with isopropyl alcohol over series of structurally related zeolites reflect a decrease with

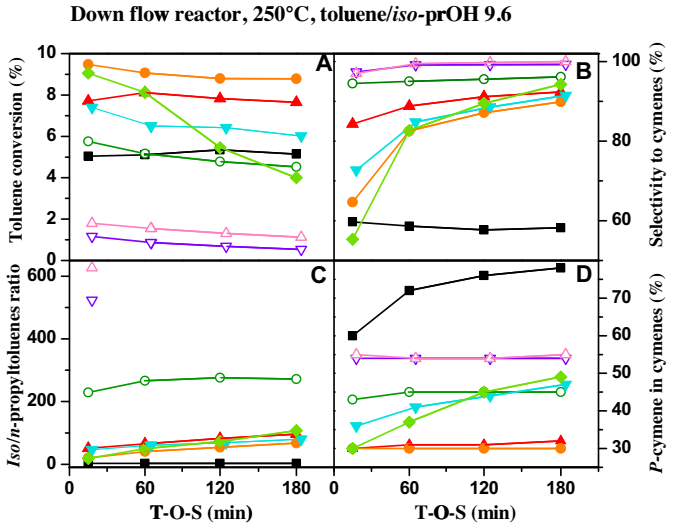

Fig. 6. Time-on-stream dependence of toluene conversion (A), selectivity to cymenes (B), *iso*-/*n*-propyltoluene ratio (C) and *para*-cymene selectivity (D) in toluene alkylation with isopropyl alcohol at 250 °C. MFI (■), BEA (●), UTL (▲), IPC-1PI (○), IPC-7 (◆), IPC-2 with Si/Al 48 (▼), IPC-6 (△), IPC-4 (▽).

decreasing channel size from 14- to 8-rings, which is due to increasing effect of diffusion constraints (Figs. 6 and 7). The highest toluene conversion was achieved for zeolite BEA followed by UTL. Three important factors influence these results, (i) zeolite BEA possesses a higher concentration of acid sites (cf. Table 2), (ii) zeolite BEA exhibits much smaller crystals in contrast to sheet-like crystals of UTL, (iii) the three-dimensional system of zeolite BEA is more easily accessible than 14-12-R system of UTL (Fig. 6A). This is in a good agreement with results of Corma tested in the catalytic cracking of *n*-decane, triisopropylbenzene, and vacuum gas oil [34]. Toluene conversion over IPC-7 decreases substantially with time-on-stream (T-O-S), which can be explained in terms of a high concentration of Lewis acid sites (Table 2) promoting deactivation of this zeolite. IPC-2 (OKO, 12-10-R channels) showed a higher conversion than IPC-1PI and MFI. Although the structure of pillared IPC-1PI and MFI are so different, both catalysts exhibited similar conversions. It should be noted that around 30% of IPC-1PI is formed by amorphous silica, thus, the concentration of acid sites is diluted in comparison with other zeolites. As it will be seen *vida infra*, despite the same conversions of MFI and IPC-1PI the selectivities of both catalysts were substantially different. The lowest conversions were achieved over IPC-6 and IPC-4 (PCR). Channel structure of IPC-6 is formed by two non-intersecting channel systems (12-10-R and 10-8-R). In IPC-6 we assume that the active sites are mostly located in the smaller 10-8-R channel system, where they are not available for aromatic molecules as proved to be the case on IPC-4 zeolite (with only 10-8-R). Therefore, the catalysis proceeded only on the external surface similarly to IPC-4. The 10-R channels in IPC-4 have distinctive elliptical shape (5.8 Å × 3.8 Å) compared to more spherical 10-R channels of MFI (5.1 Å × 5.5 Å and 5.3 Å × 5.6 Å). The 8-R channels are too small to contribute to the alkylation reaction of aromatics. This means that particularly IPC-4 (PCR) can be considered in this reaction as zeolite with one-dimensional channel system.

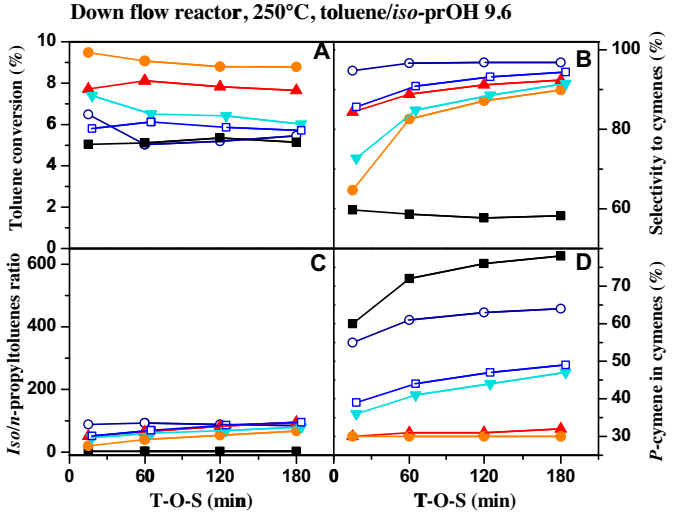

Fig. 7. Time-on-stream dependence of toluene conversion (A), selectivity to cymenes (B), *iso*-/*n*-propyltoluene ratio (C) and *para*-cymene selectivity (D) in toluene alkylation with isopropyl alcohol at 250 °C. MFI (■), BEA (●), UTL (▲), IPC-2 with Si/Al = 48 (▼), IPC-2 with Si/Al = 81 (□), IPC-2 with = Si/Al 109 (○).

Selectivities to cymenes, the primary reaction products for *o*- and *p*-cymenes and isomerization product for *m*-cymene, depend again very strongly on the size and connectivity of the zeolite channel system (Fig. 6B). In the case of MFI, selectivity to cymenes is rather constant within 180 min T-O-S at only around 60% as a result of bimolecular transalkylation between cymenes and toluene to *n*-propyl toluenes. This reaction is strongly enhanced by intersecting 10-ring channels [35,36]. In the case of IPC-1PI, IPC-4 and IPC-6, selectivity to cymenes is higher than 90% after 120 min of T-O-S. Since IPC-1PI does not possess any microporosity, the active centres are located only in the open layer surface. We assume that Al-IPC-1PI acts similar to solid acids where only cymenes are almost exclusively formed. On the other hand, acid centres in IPC-4 and IPC-6 channels are not accessible for aromatic molecules (discussion vide supra), accordingly the reaction proceeds only on the external surface (similarly to IPC-1PI). Lower selectivities for UTL, IPC-7, and IPC-2 are mostly due to secondary alkylation of primary formed cymenes or at a lesser extent toluene disproportionation.

The isopropyl (cymene)/*n*-propyl toluene ratio (Fig. 6C) is again different among individual catalysts. While the isopropyl/*n*-propyl toluene ratio is close to 2 for MFI zeolite, this value is between 70 and 100 for other zeolites after 120 min of T-O-S. In contrast, IPC-1PI without any micropores reaches the ratio about 200. The very low activity of IPC-4 and IPC-6 zeolites is responsible for almost negligible rate of this bimolecular reaction providing values around 500–600. It evidences that the steric constraints of 10-ring intersecting channels are a primary requisite for the performance of this bimolecular reaction.

Selectivity to *p*-cymene reflects primarily diffusion constraints in the channel system and first alkylation step directly providing *p*-cymene. As it is well-known from the literature [36], 10-ring MFI is the superior for the selectivity to *p*-cymene with values above 90%. Zeolites BEA and UTL form thermodynamic concentration of *p*-cymene close to 30% indicating that the rate of isomerization controls the final selectivity.

Fig. 7 provides the same relationship stressing the effect of acid sites concentrations for IPC-2 zeolite (OKO). Three IPC-2 samples with Si/Al molar ratios 48, 81 and 109 were synthesized. Fig. 7A shows that toluene conversions at 250 °C are lower than original UTL and BEA but higher than MFI. Conversions values over IPC-2 catalysts reflect the concentrations of acid sites, IPC-2 (48) > IPC-2 (81) > IPC-2 (109). As for the selectivities to mixture of cymenes, *para*-selectivity and isopropyl/*n*-propyl toluene ratio, the relationship is just opposite. With decreasing concentration of acid sites, selectivities to primary alkylation products increase, and also the *para*-selectivity increases. With decreasing aluminium content the density of acid sites decreases. Hence, the rate of subsequent reactions like bimolecular transalkylation of primarily formed cymenes to *n*-propyl toluenes decreased [36]. It can be also speculated that

Please cite this article in press as: N. Žilková, et al., The effect of UTL layer connectivity in isoreticular zeolites on the catalytic performance in toluene alkylation, Catal. Today (2015), http://dx.doi.org/10.1016/j.cattod.2015.09.033

the increase in *para*-selectivity over IPC-2 with the low concentrations of acid sites is due to restricted isomerization of primary alkylation products (*ortho*- and *para*-). Inside the channel systems alkylation to the *para* position could be enhanced because of steric reasons as channel walls might limit the accessibility of *ortho* position for isopropyl alcohol.

4. Conclusions

A series of isoreticular zeolites derived from UTL was synthesized, characterized, and tested in toluene alkylation with isopropyl alcohol. Zeolites UTL, IPC-2, IPC-4, IPC-6, and IPC-7 possess the same structure of the layers (derived from UTL zeolite) but different connectivity of the layers.

Toluene conversion and selectivities to individual products clearly reflect the channel structure (layer connectivity) and composition of catalysts under study. Toluene conversion increases with increasing size of the zeolite channels in the sequence IPC-4 < IPC-6 < IPC-2 < IPC-7 < UTL. This sequence can be related to decreasing role of diffusion constraints in 10-ring channels. UTL zeolite is less active than zeolite BEA, although it possesses 14-12-R channel system. Three-dimensional channel system of zeolite BEA and much smaller size of the crystals are critical for higher toluene conversions over zeolite BEA.

Bimolecular transformation of cymenes with toluene to *n*-propyl toluenes proceeds to a much lower extent than with MFI zeolite. Increasing concentration of active sites in IPC-2 increases the toluene conversion and it simultaneously decreases the selectivities to primary alkylation products due to the enhanced rate of consecutive reactions.

Acknowledgements

This work has received financial support from the Czech Science Foundation (Centre of Excellence P106/12/G015). S.A.K. acknowledges the support from the Ministry of Higher Education, Saudi Arabia, in establishment of the Center of Research Excellence in Petroleum Refining & Petrochemicals at King Fahd University of Petroleum & Minerals (KFUPM). The support of KFUPM is also highly appreciated. REM thanks the EPSRC for funding (EP/L014475/1 and EP/K025112/1).

References

[1] A. Corma, J. Catal. 216 (2003) 298–312.
[2] S. Al-Khattaf, S.A. Ali, A.M. Aitani, N. Zilkova, D. Kubicka, J. Cejka, Catal. Rev.-Sci. Eng. 56 (2014) 333–402.
[3] G. Bellussi, A. Carati, C. Rizzo, R. Millini, Catal. Sci. Technol. 3 (2013) 833–857.
[4] A. Corma, V.I. Costa-Vaya, M.J. Diaz-Cabanas, F.J. Llopis, J. Catal. 207 (2002) 46–56.
[5] M. Choi, K. Na, J. Kim, Y. Sakamoto, O. Terasaki, R. Ryoo, Nature 461 (2009), 246-U120.
[6] R.E. Morris, J. Cejka, Nat. Chem. 7 (2015) 381–388.
[7] S.I. Zones, Microporous Mesoporous Mater. 144 (2011) 1–8.
[8] P. Eliášová, M. Opanasenko, P.S. Wheatley, M. Shamzhy, M. Mazur, P. Nachtigall, W.J. Roth, R.E. Morris, J. Čejka, Chem. Soc. Rev. 44 (2015) 7177–7206.
[9] W.J. Roth, P. Nachtigall, R.E. Morris, P.S. Wheatley, V.R. Seymour, S.E. Ashbrook, P. Chlubna, L. Grajciar, M. Polozij, A. Zukal, O. Shvets, J. Cejka, Nat. Chem. 5 (2013) 628–633.
[10] L. Grajciar, O. Bludsky, W.J. Roth, P. Nachtigall, Catal. Today 204 (2013) 15–21.
[11] M. Trachta, P. Nachtigall, O. Bludsky, Catal. Today 243 (2015) 32–38.
[12] W.J. Roth, P. Nachtigall, R.E. Morris, J. Cejka, Chem. Rev. 114 (2014) 4807–4837.
[13] M. Mazur, P. Chlubna-Eliasova, W.J. Roth, J. Cejka, Catal. Today 227 (2014) 37–44.
[14] M. Mazur, P.S. Wheatley, M. Navarro, W.J. Roth, M. Položij, A. Mayoral, P. Eliášová, P. Nachtigall, J. Čejka, R.E. Morris, Nat. Chem. (2015), http://dx.doi.org/10.1038/NCHEM.2374.
[15] P. Chlubna-Eliasova, Y.Y. Tian, A.B. Pinar, M. Kubu, J. Cejka, R.E. Morris, Angew. Chem. Int. Ed. Engl. 53 (2014) 7048–7050.
[16] M. Shamzhy, M. Opanasenko, Y.Y. Tian, K. Konysheya, O. Shyets, R.E. Morris, J. Cejka, Chem. Mater. 26 (2014) 5789–5798.
[17] T.C. Tsai, S.B. Liu, I.K. Wang, Appl. Catal. A: Gen. 181 (1999) 355–398.
[18] S. Al-Khattaf, C. D'Agostino, M.N. Akhtar, N. Al-Yassir, N.Y. Tan, L.F. Gladden, Catal. Sci. Technol. 4 (2014) 1017–1027.
[19] M.T. Portilla, F.J. Llopis, C. Martinez, S. Valencia, A. Corma, Appl. Catal. A: Gen. 393 (2011) 257–268.
[20] J. Cejka, A. Vondrova, B. Wichterlova, G. Vorbeck, R. Fricke, Zeolites 14 (1994) 147–153.
[21] B. Wichterlova, J. Cejka, N. Zilkova, Microporous Mesoporous Mater. 6 (1996) 405–414.
[22] M.V. Shamzhy, O.V. Shvets, M.V. Opanasenko, P.S. Yaremov, L.G. Sarkisyan, P. Chlubna, A. Zukal, V.R. Marthala, M. Hartmann, J. Cejka, J. Mater. Chem. 22 (2012) 15793–15803.
[23] O.V. Shvets, N. Kasian, A. Zukal, J. Pinkas, J. Cejka, Chem. Mater. 22 (2010) 3482–3495.
[24] P. Chlubna, W.J. Roth, H.F. Greer, W.Z. Zhou, O. Shvets, A. Zukal, J. Cejka, R.E. Morris, Chem. Mater. 25 (2013) 542–547.
[25] B. Wichterlová, Z. Tvarůžková, Z. Sobalík, P. Sarv, Microporous Mesoporous Mater. 24 (1998) 223–233.
[26] E. Verheyen, L. Joos, K. Van Havenbergh, E. Breynaert, N. Kasian, E. Gobechiya, K. Houthoofd, C. Martineau, M. Hinterstein, F. Taulelle, V. Van Speybroeck, M. Waroquier, S. Bals, G. Van Tendeloo, C.E.A. Kirschhock, J.A. Martens, Nat. Mater. 11 (2012) 1059–1064.
[27] P.S. Wheatley, P. Chlubna-Eliasova, H. Greer, W.Z. Zhou, V.R. Seymour, D.M. Dawson, S.E. Ashbrook, A.B. Pinar, L.B. McCusker, M. Opanasenko, J. Cejka, R.E. Morris, Angew. Chem. Int. Ed. Engl. 53 (2014) 13210–13214.
[28] M. Kruk, M. Jaroniec, A. Sayari, J. Phys. Chem. B 101 (1997) 583–589.
[29] M. Kruk, M. Jaroniec, A. Sayari, Chem. Mater. 11 (1999) 492–500.
[30] R.L. Smith, P. Eliasova, M. Mazur, M.P. Attfield, J. Cejka, M.W. Anderson, Chem.-Eur. J. 20 (2014) 10446–10450.
[31] P. Chlubna, W.J. Roth, A. Zukal, M. Kubu, J. Pavlatova, Catal. Today 179 (2012) 35–42.
[32] H. Xu, J.G. Jiang, B.T. Yang, L. Zhang, M.Y. He, P. Wu, Angew. Chem. Int. Ed. Engl. 53 (2014) 1355–1359.
[33] X.L. Liu, N. Kasian, A. Tuel, Microporous Mesoporous Mater. 190 (2014) 171–180.
[34] J. Martinez-Triguero, M.J. Diaz-Cabanas, M.A. Camblor, V. Fornes, T.L.M. Maesen, A. Corma, J. Catal. 182 (1999) 463–469.
[35] A. Corma, M.J. Diaz-Cabanas, C. Martinez, F. Rey, in: A. Gedeon, P. Massiani, F. Babonneau (Eds.), Zeolites and Related Materials: Trends, Targets and Challenges, Proceedings of the 4th International Feza Conference, vol. 174, 2008, pp. 1087–1090.
[36] B. Wichterlova, J. Cejka, J. Catal. 146 (1994) 523–529.

Please cite this article in press as: N. Žilková, et al., The effect of UTL layer connectivity in isoreticular zeolites on the catalytic performance in toluene alkylation, Catal. Today (2015), http://dx.doi.org/10.1016/j.cattod.2015.09.033